Journal of Naval Sciences and Engineering
2024, Vol. 20, No. 2, pp. 163-189 *DOI: 10.56850/jnse.1496134*
Electrical-Electronics Engineering/Elektrik-Elektronik Mühendisliği

RESEARCH ARTICLE

**An ethical committee approval and/or legal/special permission has not been required within the scope of this study.*

PERFORMANCE ANALYSIS OF ADAPTIVE MIMO TECHNIQUES FOR ANGULAR DIVERSITY RECEIVER-BASED VISIBLE LIGHT COMMUNICATION

Kardelen HORUNLU [1]
Yasin ÇELİK [2*]

[1] *Aksaray University, Department of Electrical and Electronics Engineering, Aksaray, Turkey, kardelenhrnlu@gmail.com*

[2] *Aksaray University, Department of Electrical and Electronics Engineering, Aksaray, Turkey, yasincelik@aksaray.edu.tr*

Received: 05.06.2024 **Accepted: 15.10.2024**

ABSTRACT

Correlation between the channels is the primary factor that restricts data rates in multiple-input multiple-output visible light communications (MIMO-VLC). Different receiver designs have been proposed to reduce this correlation value, while adaptive modulations that perform better under the correlated channel effect have been studied on the transmitter side. In this study, we conducted a performance analysis of MIMO-VLC systems by utilizing adaptive MIMO modulations at the transmitter side and angular diversity receiver (ADR) structures at the receiver side. As adaptive modulations, created using spatial diversity (SD) and spatial multiplexing (SMP) modulations, SD/SMP switching, adaptive SMP (aSMP), and SD-assisted adaptive SMP (SD-aSMP) are considered. Analytical and simulation results were obtained for achievable data rates in an indoor environment. Cumulative distribution function (CDF) graphs were used to assess the overall performance based on these data rates. GADR has an advantage over ADR in low SNR regions but performs similarly in high SNR regions. The SD-aSMP scheme demonstrated the best performance across all SNR regions as a hybrid modulation, taking advantage of diversity gain in low SNR and multiplexing gain in high SNR regions. The adaptive SMP schemes benefit from increasing the number of LEDs and increasing the elevation angle up to 60 degrees.

Keywords: *Visible Light Communication (VLC), Angular Diversity Receiver (ADR), Multiple-Input Multiple-Output (MIMO).*

AÇISAL ÇEŞİTLEMELİ ALICI TABANLI GÖRÜNÜR IŞIK HABERLEŞMESİ İÇİN UYARLANABİLİR MIMO TEKNİKLERİNİN PERFORMANS ANALİZİ

ÖZ

Kanallar arası ilinti çok-girişli çok-çıkışlı görünür ışık haberleşmesinde (MIMO-VLC) veri hızlarını sınırlayan en büyük etkendir. Bu ilinti değerini azaltmak için farklı alıcı tasarımları önerilmiştir. Diğer taraftan ilintili kanal etkisi altında daha iyi performans gösteren uyarlanabilir modülasyonlar verici tarafta çalışılmıştır. Bu çalışmada, verici tarafta uyarlanabilir MIMO modülasyonları ve alıcı tarafta açısal çeşitlemeli alıcı (ADR) yapıları kullanılarak MIMO-VLC sistemlerin performans analizi yapılmıştır. Uyarlanabilir modülasyonlar olarak uzamsal çeşitleme (SD) ve uzamsal çoğullama (SMP) modülasyonları kullanılarak oluşturulan; SD/SMP anahtarlaması, uyarlanabilir SMP (aSMP) ve SD-destekli uyarlanabilir SMP (SD-aSMP) dikkate alınmıştır. Bina içi ortamda ulaşılabilir veri (AR) hızlarının analitik ve benzetim sonuçları elde edilmiştir. AR değerleri kullanılarak bina içi ortamın genelindeki performansları değerlendirebilmek için toplamsal dağılım fonksiyonu (CDF) grafikleri çizdirilmiştir. GADR, düşük SNR bölgelerinde ADR'ye göre avantajlıdır ancak yüksek SNR bölgelerinde benzer şekilde performans gösterir. SD-aSMP şeması, düşük SNR'de çeşitlilik kazancından ve yüksek SNR bölgelerinde çoğullama kazancından yararlanarak hibrit bir modülasyon olarak tüm SNR bölgelerinde en iyi performansı göstermiştir. LED sayısının arttırılması uyarlanabilir SMP şemalarının performansını artırmıştır. Benzer şekilde yükseklik açısının 60 dereceye kadar arttırılması da uyarlanabilir SMP şemalarının performansını iyileştirmiştir.

Anahtar Kelimeler: *Görünür Işık Haberleşmesi (VLC), Açısal Çeşitlemeli Alıcı (ADR), Çok-Girişli Çok-Çıkışlı Sistemler (MIMO).*

1. INTRODUCTION

The Internet of Things (IoT) is a rapidly emerging field, and its networks need to be able to transmit data at high densities and speeds indoors. Radio frequency (RF) technologies are often used for wireless communication in indoor environments. Electromagnetic interference (EMI), limited spectrum, and low power efficiency are some existing problems for radio frequency (RF) devices (Zhang, et al., 2020). In recent years, visible light communication (VLC) has gained attention as an alternative technology to solve the abovementioned issues for short-range indoor places. In addition to offering secure data transfer and lighting simultaneously, VLC provides the benefits of being inexpensive, energy-efficient, and having a huge unregulated spectrum. With these advantages, VLC is a standout auxiliary technology that is suggested for new-generation wireless networks (Armstrong et al., 2013). Phase information is not used in VLC; data transfer only happens via the signal's amplitude information. Intensity modulation direct detection (IM/DD) is the term used to describe this type of communication. High-speed communication is restricted by the electrical bandwidth of a few Megahertz (MHz) in VLC, despite the accessible optical bandwidth being 400 Terahertz (THz) (Alsabah et al., 2021). The studies in the VLC field, which were put forward in the early 21st century, gained momentum with the concept of Light Fidelity (Li-Fi), announced by German scientist Harald Haas in 2011. Li-Fi is a wireless communication and network system transmitting two-way data at high speeds over visible light, ultraviolet, and infrared spectrums. In this system, light-emitting diodes (LEDs) are used as transmitters, and photodetectors (PDs) are used as receivers (Tsonev et al., 2014). However, optical camera communication (OCC), which uses a camera on the receiver side to transmit data at lower speeds, has emerged as a different type of VLC (Luo et al., 2015).

Wireless communication systems with more than one antenna at the receiver and transmitter have greatly improved performance compared to single-antenna systems, which has attracted a lot of attention in new generations (Guo, et al. 2021). Multiple LEDs are typically set on the ceiling to create an interior space with uniform and sufficient lighting. This inherently facilitates multiple-input multiple-output (MIMO) transmission in VLC systems (Zeng et al., 2009). Consequently, there has been a growing interest in MIMO-VLC research over the past decade. Three MIMO schemes—spatial modulation (SM), spatial diversity (SD) or Repetition Coding (RC), and spatial multiplexing (SMP)—are typically evaluated in the majority of MIMO-VLC systems (Fath & Haas, 2013). Furthermore, enhanced MIMO transmission techniques have been proposed for a significant boost in MIMO-VLC system efficiency, including user-centric MIMO and index-modulated MIMO approaches. A unique approach to index-modulated MIMO-VLC systems using orthogonal frequency division multiplexing (OFDM) was introduced in 2017 (Yesilkaya et al., 2017). The suggested method eliminates the common bandwidth losses in OFDM signals caused by time- and frequency-domain shaping. This is accomplished by utilizing LED index modulation in conjunction with spatial multiplexing. GLIM-OFDM's drawbacks, however, are receiver complexity and illumination constraints.

The user-centered performance of the planar receiver structure, whose photodetectors (PD) are placed at a fixed 90-degree angle toward the ceiling, was examined in 2020 (Chen et al., 2020). In that paper, the achievable rate has been investigated for three user-centric MIMO techniques: adaptive SMP (aSMP), SD/SMP switching, and SD-assisted aSMP (SD-aSMP) to increase performance in indoor MIMO-VLC systems. Users' indoor locations are exploited as a new degree of diversity. However, the correlation between channels is high since all PDs have the same orientation in the receiver structure. Furthermore, the deployment of LEDs, which significantly impacts MIMO performance and channel correlation, was neglected (Vegni & Biagi 2019).

In recent years, angular diversity transmitters (ADT) have been proposed for optical attocell networks (Chen et al, 2017). The ADT's use of space division multiple access (SDMA) in these networks resulted in improved area spectrum efficiency compared to conventional time division multiple access (TDMA) (Dixit & Kumar 2020). ADTs are utilized to improve the performance of MIMO-VLC systems, which are designed to include one central LED and multiple angled side LEDs (Qin et al, 2022). However, angular diversity transmitters have limitations regarding indoor lighting uniformity.

MIMO communication has the ability to improve VLC performance, but in real-world VLC systems, its performance increase is still quite small. This is mostly because of the strong correlation between channels that results from the narrow receiver spacing in the planar receiver types (Fath & Haas, 2013). Several approaches have been proposed in the literature to address the high correlation problem between channels in MIMO-VLC systems in which angle diversity receiver

(ADR) is the most effective solution among them (Nuwanpriya et al, 2014). The use of directional PDs significantly reduces the correlation of the channel matrix in MIMO-VLC systems compared to the planar receiver. A pyramid-type ADR structure was proposed and its advantages over planar receivers were examined (Nuwanpriya et al., 2015). In this structure, there are 4 PDs placed on the surfaces of the pyramid. Horizontal rotation (azimuth) and vertical increment (elevation) angles are available as the parameters in the ADR structure. These angles respectively give the rotation angle of the receiver relative to the x-axis in the x-y plane and the elevation angle of the lateral surfaces of the pyramid from the ground.

The generalized ADR (GADR) structure includes a 5th planar PD placed at the top of the pyramid in addition to the ADR structure (Celik, 2023). The GADR structure is referred to as frustum type ADR in certain academic papers. The performance analysis of a MIMO-VLC scheme employing the ADR is detailed for downlink (Harada et al., 2023). Four distinct ADR setups with varying numbers of PDs were modeled. Through analytical analysis and simulation, the effectiveness of each ADR was demonstrated. An analysis of the network's multi-stream coverage in an indoor mobile scenario revealed that an ADR with more PDs may handle more streams to a target BER. Furthermore, it is demonstrated that the frustum type ADR offers superior coverage.

The data rates achievable by user-centric (UC) transmission techniques using ADR and GADR models have been determined for MIMO-VLC wireless systems in 2024 (Horunlu & Celik 2024). The user-centered structure is achieved using SD/SMP, aSMP, and SD-aSMP MIMO transmission schemes considering the channel between the receiver and the transmitter. However, they only considered the classical *4x4* and *4x5* MIMO and did not expand on the results for receiver parameters. In recent days, a user-centric access point (AP) clustering strategy built for indoor VLC networks is presented in order to address the growing demands for high data speeds in VLC. A stable pairing connects the VLC user equipments (UEs) and access points (APs), and the overall optimization goal is to maximize the total achievable system ratio (SASR). Additionally, an analysis of the suggested mechanism's efficiency, stability, convergence, and complexity is carried out (Su et al., 2024). However, as the pairing space grows, the suggested system's complexity rises exponentially.

Channel structure and correlation in MIMO-VLC systems are highly dependent on the location of users. As mentioned above, studies have addressed this issue and proposed new transmission techniques, receiver types, and LED deployments (Vegni & Biagi 2019; Chen et al., 2020; Nuwanpriya et al., 2015; Harada et al., 2023). Joint performance analysis of these strategies has not yet been taken into consideration, though. In this paper, changing the number of LEDs, changing the number of PDs, and changing the angle parameters of the ADR receiver were analyzed in detail through simulation and analytical results. The lowest achievable data rates were calculated using the cumulative distribution function (CDF) for a specific portion of indoor spaces. This work enhances data rates in indoor environments with correlated channels by employing innovative MIMO concepts based on users' spatial locations. The ADR structure is also used to reduce optical channel correlation, and optimized parameters for the receiver are analyzed.

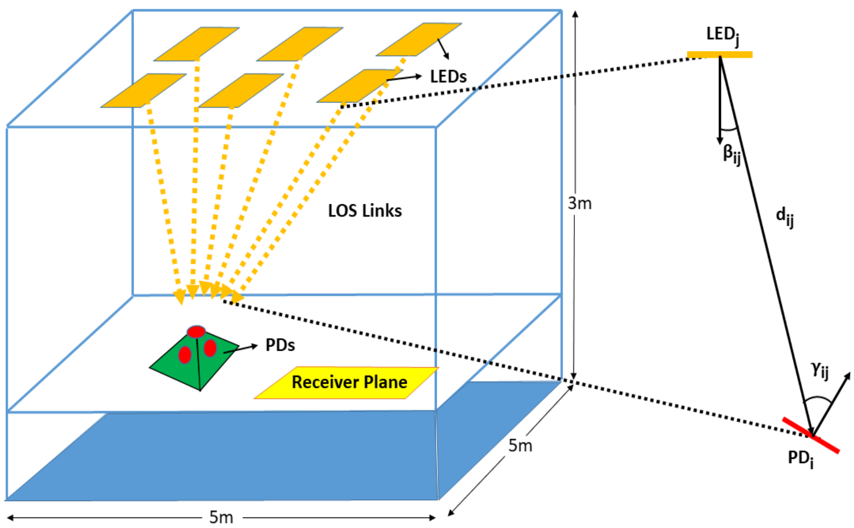

Figure 1. *Room and link geometry for MIMO-VLC system.*

2. SYSTEM MODEL

2.1. Indoor Geometry and Channel

The geometry of the MIMO-VLC system, created with LED arrays oriented at a *90-degree* angle to the floor of the room, is shown in Figure 1. The number of LED arrays is considered as N_t. The receiver is thought to be placed parallel to the floor of the room at table height. The condition $N_r \geq N_t$ is satisfied as a requirement of the SMP scheme. The height of the PDs from the ground is thought to be 0.85 m. The position of the receiver module on two axes, x and y, varies according to user mobility, which is limited to indoor space.

Due to its efficiency in mitigating intersymbol interference (ISI) resulting from dispersive channels, OFDM is widely employed in wideband wireless communication networks. Therefore, it is a good option for optical systems. However, OFDM cannot be directly applied to intensity modulation and direct detection (IM/DD) systems used in optical communications (Armstrong & Schmidt 2008). In these systems, the baseband transmitting signal changes the intensity rather than the amplitude and phase of the optical frequency carrier. Therefore, the output signal at the transmitter must be positive and real. If the input vector of the inverse fast Fourier transform (IFFT) is Hermitian symmetric, a real OFDM signal can generated. One of the two ways to make the signal positive is to apply a DC bias such as DC bias optical OFDM (DCO-OFDM) (Armstrong 2009). DCO-OFDM scheme is considered in this study. Thus, the transmitting signal vector from the LEDs consists of two components; AC signal vector $\boldsymbol{x}$ and DC bias. Since the DC bias signal has no information and is eliminated at the receiver, the received information signal is obtained as follows (Chen et al., 2020);

$$\boldsymbol{y} = \boldsymbol{H}\boldsymbol{x} + \boldsymbol{n}, \tag{1}$$

where $\boldsymbol{n} = [\, n_1, n_2, \ldots, n_{Nr} \,]^T$ is the vector modeled as additive white Gaussian noise (AWGN). The elements of $\mathbf{n}$ have a normal distribution with zero mean and σ^2 variance, $\boldsymbol{n} \sim \boldsymbol{\mathcal{N}}(0, \sigma^2)$. $\boldsymbol{x} = [\, x_1, x_2, \ldots, x_{Nt} \,]^T$ is the transmitted data vector and $\boldsymbol{y} = [\, y_1, y_2, \ldots, y_{Nr} \,]^T$ is the received vector. $\boldsymbol{H}$ represents the $N_r \times N_t$ channel matrix. The elements of ***H*** are coefficients of the line of sight (LOS) link. According to the Lambertian formula channel coefficient between the j[th] LED and the i[th] PD is given as follows (Tanaka, et al., 2001);

$$h_{ij} = \frac{(m+1)\rho A}{2\pi d_{ij}^2} cos(\beta_{ij}) \cos(\gamma_{ij}) T_s(\gamma) G(\gamma) \ , \tag{2}$$

where ρ denotes the responsivity of the PD and A is the active area. $i = 1, 2, \ldots, N_r$ and $j = 1, 2, \ldots, N_t$. d_{ij} represents the distance between the j[th] LED and the i[th] PD. β and γ are the angle of irradiance and angle of incidence, respectively. The Lambertian order coefficient, m, is obtained as follows;

$$m = \frac{-ln ln\,(2)}{ln\,(cos\,(\Psi))}, \tag{3}$$

where Ψ is the semiangle of the LED at half power. $G(\gamma)$ and $T_s(\gamma)$ are the optical coefficients of the lens and the filter at the receiver, respectively. $G(\gamma)$ is obtained with an idealized PD with an internal refractive index of n_{RI} as follows (Kahn & Barry 1997);

$$G(\gamma) = \frac{n_{RI}^2}{\psi_c}, \tag{4}$$

where ψ_c refers to the half-angle field of view (FOV), a special angle for PDs. Photon activates current on the PD if its angle of incidence is equal to or smaller than the FOV. Finally, if the angle between the beam and the receiver normal is greater than the FOV angle, the channel coefficient, h_{ij}, is obtained as 0.

Equation (1) clarifies that the electrical signal at the output of each PD is a linear sum of its input signal and additive noise. Since MIMO demultiplexing at the receiver side can be readily accomplished in real-world VLC systems without requiring the adjustment of LED input electrical powers, it is used here to recover the input signals effectively. Numerous MIMO demultiplexing methods have been presented, including vertical Bell Labs layered space-time, minimum mean-square error (MMSE), and zero-forcing (ZF) (Gesbert 2003). ZF has been used extensively in MIMO-VLC systems because of its ease of use and little computational complexity (Chen et al., 2020). Therefore, in the study that follows, we use ZF-based MIMO demultiplexing.

The proposed MIMO-VLC system channel matrix $\boldsymbol{H}$ is full-rank. This requirement is met provided $N_r \geq N_t$. Therefore, $\boldsymbol{H}^{\dagger}$ is obtained as the pseudo inverse of $\boldsymbol{H}$ and evaluated as follows (Penrose 1955);

$$\boldsymbol{H}^{\dagger} = (\boldsymbol{H}^{*}\boldsymbol{H})^{-1}\boldsymbol{H}^{*}. \tag{5}$$

The estimated data vector, $\hat{\boldsymbol{x}}$, is obtained by multiplying the received signal with the pseudo-inverse of the channel matrix as follows (Gesbert 2003);

$$\hat{\boldsymbol{x}} = \boldsymbol{H}^{\dagger}\boldsymbol{y} = \boldsymbol{x} + \boldsymbol{H}^{\dagger}\boldsymbol{n}. \tag{6}$$

2.2. Receiver Modules

Two different receiver types were considered in this study. The first is Polygonal Pyramid ADR, which has (N_r -1) PDs on polygonal surfaces. The GADR receiver module consists of one PD in the center, oriented at a 90-degree angle to the ceiling of the room, and (N_r -1) PDs on the polygonal surfaces (Nuwanpriya et al, 2014).

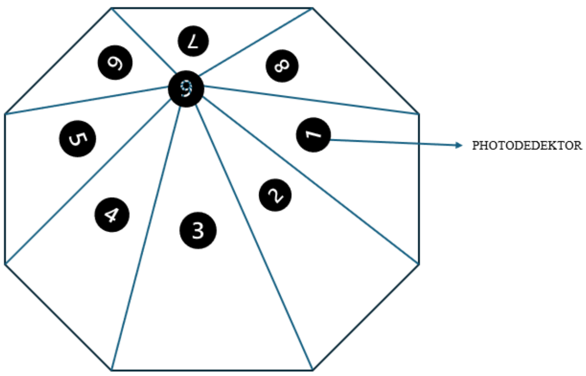

Figure 2. *GADR with 9 PDs.*

ADR and GADR have a compact structure and are easy to assemble. As a result of the compact form, there are roughly equal distances between the PDs and the same

LED. The receiver's basic concept is adjusting each PD's normal vector so that varied incident angles from the same LED result in different channel gains. Therefore, the correlation between channels decreases in the MIMO system.

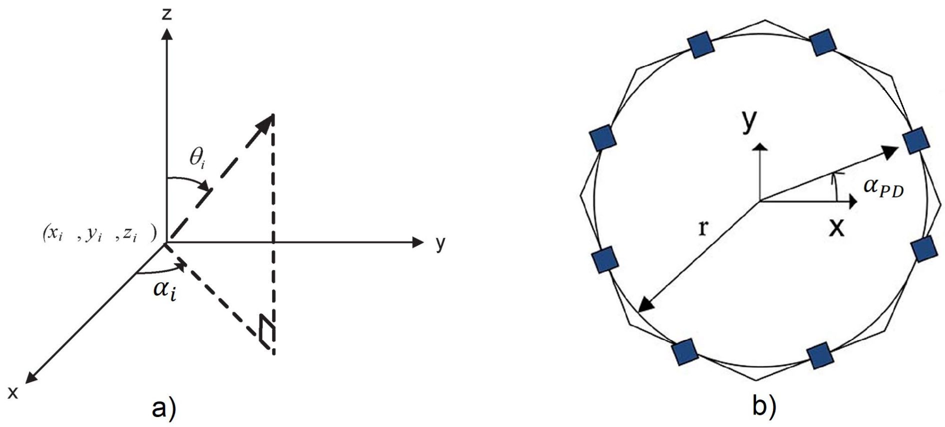

Figure 3. *a) Azimuth and Elevation angles, b) PD arrangement on the horizontal plane.*

A PD is installed on each triangle surface of the ADR, which is built in a straightforward manner that resembles a pyramid with an equilateral (N_r-1)-gon base. Unlike ADR, the normal of the N^{th} PD on GADR is perpendicular to the horizontal plane and is oriented with its face upward in the center. As a result, the PDs' normal vectors in the ADR and GADR point in various directions. Figure 2 shows an example of a GADR with N=9. We assume that the PDs are situated at a height of h_{PD} on a horizontal plane. The coordinate of the i^{th} PD on the i^{th} triangle surface is obtained as follows;

$$x_{PD}^{i} = x_{PD} + rcos\left(\frac{2(i-1)\,\pi}{N-1}\right), y_{PD}^{i} = y_{PD} + rsin\left(\frac{2(i-1)\,\pi}{N-1}\right),\ z_{PD}^{i} \ = h_{PD}, \quad (7)$$

where r is the radius of the circle tangent to the polygon at the base of the ADR and GADR structure. Each PD has an elevation angle equal to θ, a parameter that must be defined. In other words, $\theta_i = \theta$ for $i \in \{1, \cdots, (N-1)\}$. On the other hand, the azimuth angle of the i^{th} PD, α_i is given by;

$$\alpha_i = \frac{2(i-1)\,\pi}{N-1} + \alpha_{PD} \quad (8)$$

The normal vectors of the LEDs and PDs are expressed in the format [*x, y, z*, α, θ], where (*x, y, z*) represents the Cartesian coordinates of the vector's origin, and $\theta \in[0, \pi]$ and $\alpha \in[0, 2\pi]$ represent the angles from the positive z-axis (i.e., the elevation angle), and the positive x-axis (i.e., the azimuth angle), respectively.

3. METHODOLOGY

The highest data rate that may be sent over a MIMO system with an infinitely low error rate is known as its capacity. The mutual information equation for a SISO channel is extended to determine the capacity of a MIMO channel (Telatar 1999);

$$C = \ [H(\boldsymbol{Y}) - H(\boldsymbol{Y}|\boldsymbol{X})]. \tag{9}$$

In this context, *H(***Y***)* and *H(***Y**|**X***)* represent the entropy of **y** and the conditional entropy of **y** given **x**, respectively. The term *p(***x***)* denotes the input distribution. The maximization of *p(***x***)* for the AWGN channel is Gaussian and provides the channel capacity in bits/s as follows (Shannon 1948);

$$C = Blog_2(1 + \Gamma). \tag{10}$$

The signal-to-noise ratio (SNR), Γ, is P_s/P_n. Where P_s is the transmitted signal power and P_n is the noise power. Here P_n is defined as the N_0B, where *B* is the modulation bandwidth and N_0 is the noise power spectral density (PSD). The achievable rate, *R*, is the transmitted bits in unit time and bandwidth, i.e., spectral efficiency (bit/s/Hz), hence *R = C/B*.

3.1. The Achievable Rate of the SD

For VLC channels, it is quite easy to get a reasonable estimate of $\boldsymbol{H}$, hence it is assumed that the receiver knows the MIMO channel matrix. Since all LEDs send the same signal in the SD scheme, the SNR at the i^{th} PD output is calculated as follows;

$$\Gamma_{i,SD} = \left(\sum_{j=1}^{N_t} h_{ij}\right)^2 \Gamma. \tag{11}$$

The achievable rate of SD is determined concerning the received SNR, Γ_{SD}, which is derived according to the technique used at the receiver. Maximum ratio combining

(MRC) is the best receiver approach for SD. Therefore, Γ_{SD} is the sum of the output SNRs of all PDs (Chen et al., 2020).

$$\Gamma_{SD} = \sum_{i=1}^{N_r} \left(\sum_{j=1}^{N_t} h_{ij}\right)^2 \Gamma. \tag{12}$$

According to Eq. (10) and $R = C/B$, the achievable rate of the SD scheme with DCO-OFDM signaling is obtained as follows;

$$R_{SD} = \frac{1}{2}(1 + \Gamma_{SD}) . \tag{13}$$

The *1/2* multiplier comes from the two-fold bandwidth usage of the DCO-OFDM signal.

3.2. The Achievable Rate of the SMP

Unlike the SD technique, SMP requires demultiplexing at the receiver side because it sends independent symbols from the LEDs. The pseudo-inverse of the channel matrix, $\boldsymbol{H}^{\dagger}$, achieves the demultiplexing at the receiver. After that, the SNR of the received signal from the l^{th} LED is calculated as follows;

$$\Gamma_{l,SMP} = \frac{\Gamma}{\left(\sum_{r=1}^{N_r} \tilde{h}_{tr}^2\right)}, \tag{14}$$

where $\tilde{h}_{tr}$ is the coefficient from the t^{th} row and the r^{th} column of $\boldsymbol{H}^{\dagger}$. The achievable rate of an SMP system with $N_r x N_t$ size and DCO-OFDM signaling is obtained as follows (Chen et al., 2020);

$$R_{SMP} = \frac{1}{2} \sum_{t=1}^{N_t} \left(1 + \Gamma_{l,SMP}\right) . \tag{15}$$

Due to the correlation of channels, the channel matrix seriously affects the SMP capacity.

3.3. Adaptive MIMO Schemes

A mobile user in an indoor environment experiences different channel correlations for MIMO-VLC systems as they move around the room. Therefore, an adaptive scheme has more advantages than SD and SMP. According to the changes in the correlation of channels, the MIMO scheme can achieve larger capacity by choosing strong paths to send signals. Using SD and SMP together or switching between them is more efficient for MIMO-VLC. Since the correlation change of the channel depends on the user's location, adaptive modulations can also be called user-centric (Chen et al., 2020).

3.3.1. The Achievable Rate of the SD/SMP Switching Scheme

One of the adaptive MIMO schemes is SD/SMP switching. This method dynamically switches the MIMO mode between SMP and SD. LEDs transmit multiple data streams in SMP mode, while in SD mode all LEDs transmit the same data stream. This transition dynamic is taken advantage of to increase capacity. Consequently, the SD/SMP switching MIMO-VLC system's achievable rate is calculated as follows;

$$R_{SD/SMP} = \begin{Bmatrix} R_{SD} & if \;\; R_{SD} \geq R_{SMP} \\ R_{SMP} & if \;\; R_{SD} < R_{SMP} \end{Bmatrix}. \tag{16}$$

3.3.2. The Achievable Rate of the aSMP Scheme

In traditional SMP, all LEDs send signals without considering the receivers' locations. However, taking advantage of these locations can create a new degree of diversity. In aSMP, only a particular subset of LEDs is enabled to transmit independent data streams, while the others are used for illumination purposes only. The system is utilized more effectively in this way and the achievable rate increases. Assume that the number of LEDs activated is N_k, which must be less than or equal to N_t. In that case, the corresponding channel matrix is defined as follows;

$$\boldsymbol{\Lambda}_{N_r x N_k} = \left[\boldsymbol{\lambda}_1, \boldsymbol{\lambda}_2, \dots, \boldsymbol{\lambda}_{N_k}\right] = \left[\boldsymbol{\lambda}_{11} \cdots \boldsymbol{\lambda}_{1N_k} \vdots \ddots \vdots \boldsymbol{\lambda}_{N_r1} \cdots \boldsymbol{\lambda}_{NrN_k}\right]. \tag{17}$$

Following that, the SNR of the received signal from the l^{th} active LED is calculated as follows;

$$\Gamma_{l,aSMP} = \frac{\Gamma}{\left(\sum_{r=1}^{N_r} \tilde{\lambda}_{tr}^{2}\right)}, \tag{18}$$

where $\widetilde{\boldsymbol{\lambda}}_{tr}$ is the coefficient from the t^{th} row and the r^{th} column of $\boldsymbol{\Lambda}^{\dagger}$ which is the pseudo-inverse of Λ. Using Eq. (15) the achievable rate of an aSMP system is given by;

$$R_{aSMP} = \frac{1}{2} \sum_{t=1}^{N_k} \left(1 + \Gamma_{l,aSMP}\right). \tag{19}$$

The basic idea of implementing aSMP is to select the subset of LEDs that provide signal transmission that maximizes the achievable rate of the MIMO-VLC system. A detailed procedure of LED subset selection in aSMP is given in the reference (Chen et al., 2020).

3.3.3. The Achievable Rate of the SD-aSMP Scheme

Unlike aSMP, the SD-aSMP scheme involves using disabled LEDs for transmission. This increases resource utilization, allowing the LEDs ignored in aSMP to contribute to the SNR increase at the receiver. The main purpose of this technique is to increase the resistance of a link to noise by obtaining additional diversity gain in the MIMO structure.

It is assumed here that the disabled LEDs transmit the same symbol as the active LED away from the user. Thus, the added diversity gain can effectively increase the gain of the signal emitted by the outermost LED and reduce the negative effect of noise amplification compared to an aSMP. Considering that, N_k LEDs are used to transmit different symbols and the z^{th} LED is the outermost LED from the user. In this case, the channel matrix for these N_k LEDs can be denoted as in Eq. (17), which is given by;

$$\boldsymbol{\Lambda}_{N_r x N_k} = \left[\boldsymbol{\lambda}_1, \boldsymbol{\lambda}_2, \ldots, \boldsymbol{\lambda}_z, \ldots, \boldsymbol{\lambda}_{N_k}\right]. \tag{20}$$

On the other hand, (N_t - N_k) LEDs are used to transmit the same symbol as the z^{th} LED, and the channel matrix obtained for SD-aSMP can be expressed as follows;

$$\boldsymbol{W}_{Nr \times N_k} = \left[\boldsymbol{w}_1, \boldsymbol{w}_2, \ldots, \boldsymbol{w}_z, \ldots, \boldsymbol{w}_{N_k}\right], \tag{21}$$

where $\boldsymbol{w}_i = \boldsymbol{\lambda}_i$, *i=1,2,..,N*$_k$, except $\boldsymbol{w}_z$. $\boldsymbol{w}_z = \boldsymbol{\lambda}_z + \sum_{j=N_k+1}^{N_t} \boldsymbol{\lambda}_j$. After that, the SNR of the received signal from the l^{th} active LED is calculated as follows (Chen et al., 2020);

$$\Gamma_{l,SD-aSMP} = \frac{\Gamma}{\left(\sum_{r=1}^{N_r} \widetilde{w}_{tr}^2\right)}, \tag{22}$$

where $\widetilde{\boldsymbol{w}}_{tr}$ is the coefficient from the t^{th} row and the r^{th} column of $\boldsymbol{W}^{\dagger}$ which is the pseudo-inverse of $\boldsymbol{W}$. Using Eq. (15) the achievable rate of an SD-aSMP system is given by;

$$R_{SD-aSMP} = \frac{1}{2} \sum_{t=1}^{N_k} \left(1 + \Gamma_{l,SD-aSMP}\right). \tag{23}$$

N_k value is determined by taking into account the channel matrix, **H**. Finally, the procedure of optimal LED subset selection in SD-aSMP is given in the reference (Chen et al., 2020).

4. SIMULATIONS

In this study, to evaluate the performance of the indoor adaptive MIMO-VLC system, the achievable data rates obtained with ADR and GADR receivers are plotted. Performances were determined concerning SNR in different positions in the quarter section of the room. Moreover, the analytical and simulation results were obtained separately and agreed well. Additionally, to interpret how the achievable data rates vary for different MIMO schemes in the indoor space, the results in the entire room were gathered and CDF graphs were created. All simulation parameters are given in Table 1.

Receiver positions from *Position 1* to *Position 6* are considered to establish achievable rate performances of MIMO-VLC. Only one-quarter of the room was selected for symmetry reasons; The same performances will also be achieved in other quarters. Consequently, the receiver x-y positions from *Position 1* to *Position 6* are (0.5 - 0.5), (1.5 - 0.5), (1.5 - 0.5), (2.5 - 0.5), (2.5 - 1.5), (2.5 - 2.5), (1.5 - 1.5), respectively.

Table 1. *Simulation Parameters.*

Parameter	Value
Room length (X)	5 m
Room width (Y)	5 m
Room height (Z)	3 m
No. of transmitters (N_t)	4, 5, 8, 9, 12, 16
No. of receivers (N_r)	5, 6, 9, 10, 13, 17
Elevation of the LEDs	-90°
Azimuth of the LEDs	0°
Semi-angle at half power (Ψ)	70°
Optical gain of the filter G(γ)	0.9
Refractive index of the lens	1.5
Field of view of the PD (FOV)	70°
PD height from the floor	0.85 m
Responsivity (ρ)	0.53 A/$\sqrt{W}$
Active area of the PD (A)	1 cm^2
Azimuth of the PD	180° /(N_r-1)
Elevation of the PD	30°, 45°, 60°, 75°
Modulation bandwidth	20 MHz
PSD of Noise	10^{-22} A^2/Hz
FFT size	128
Constellation	BPSK

In simulations, we take account of an $N_r \times N_t$ MIMO-VLC system and an indoor environment with a dimension of *5 m × 5 m × 3 m*. The LEDs are mounted on the ceiling and the user with ADR or GADR is positioned inside the receiving plane with a height of *0.85 m*. Table 1 lists the essential simulation parameters. The position of the LEDs varies depending on how many are used. The x-y positions of the LEDs for different setups are given in Table 2.

Table 2. *x-y positions of LEDs.*

N_t	x-y positions (m)
4	{1.25-1.25; 1.25-3.75; 3.75-1.25; 3.75-3.75}
5	{1.03-1.03; 3.96-1.03; 2.50-2.50; 1.03-3.96; 3.96-3.96}
8	{0.85-0.85; 4.14-0.85; 2.50-1.29; 1.29-2.50; 3.70-2.50; 2.50-3.70; 0.85-4.14; 4.14-4.14}
9	{0.83-0.83; 2.50-0.83; 4.16-0.83; 0.83-2.50; 2.50-2.50; 4.16-2.50; 0.83-4.16; 2.50-4.16; 4.16-4.16}
12	{0.70-0.70; 3.10-0.70; 1.90-1.46; 4.29-1.46; 0.70-2.12; 3.10-2.12; 1.90-2.87; 4.29-2.87; 0.70-3.54; 3.10-3.54; 1.90-4.29; 4.29-4.29}
16	{0.62-0.62; 1.87-0.62; 3.12-0.62; 4.37-0.62; 0.62-1.87; 1.87-1.87; 3.12-1.87; 4.37-1.87; 0.62-3.12; 1.87-3.12; 3.12-3.12; 4.37-3.12; 0.62-4.37; 1.87-4.37; 3.12-4.37; 4.37-4.37}

4.1. Achievable Rate Performances

In Figure 4, we examined the achievable rates of MIMO schemes for different receivers in a four-LED indoor MIMO-VLC system. The receivers considered here are ADR, GADR, and planar receiver. For the planar receiver, the distance between PDs was assumed to be 10 cm and the elevation angle was selected as 35 degrees for ADR and GADR. The receiver's position in the *x-y* plane was chosen as (1.5, 0.5). Marks and lines represent simulation and analytical results, respectively. As can be seen, the simulations agree well with the analytical results. GADR has an advantage over ADR in low SNR regions but performs similarly in high SNR regions. Here, the diversity gain contribution of the PD at the top of the receiver is effective. In the high SNR region where multiplexing gain dominates, GADR and ADR performances approach each other. The SD-aSMP scheme with GADR outperforms all other schemes for low and high SNR regions. As a hybrid modulation, SD-aSMP takes advantage of diversity gain in the low SNR region and multiplexing gain in the high SNR region. Since the decreasing channel correlation improves the performance of SMP variations, achievable rates of SD-aSMP, aSMP, SMP, and SD/SMP differ significantly from the others in the high SNR region, especially for ADR and GADR. SMP with planar receiver has the worst performance.

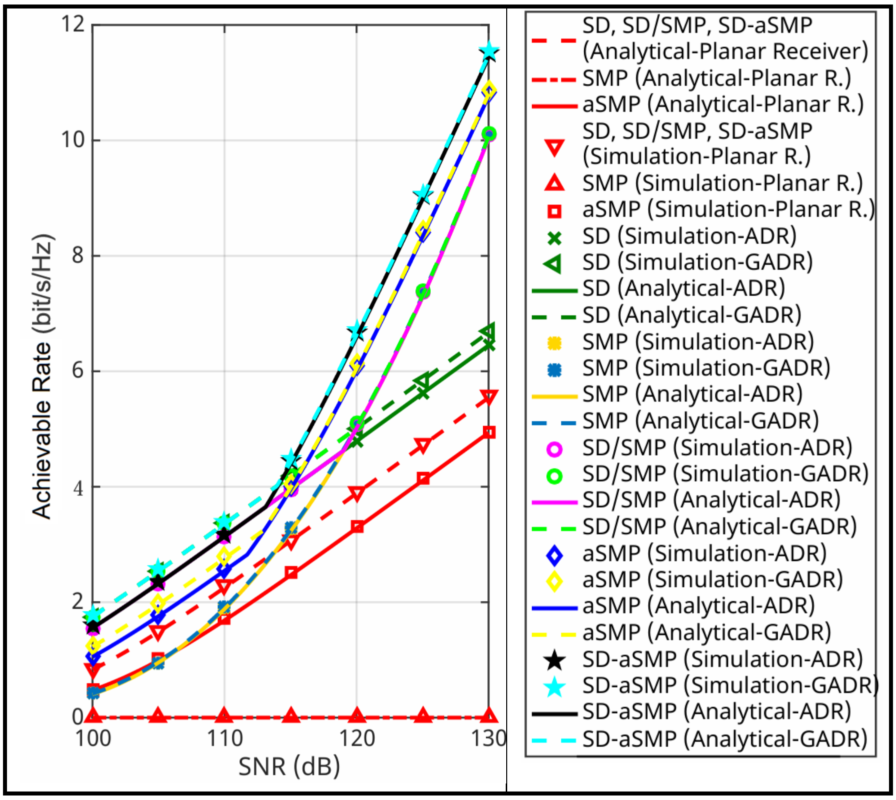

Figure 4. *Achievable rates of 4x4 and 4x5 MIMO-VLC schemes considering all receivers at Position 2.*

In Figure 5, the receiver's position in the *x-y* plane was chosen as (2.5, 2.5), the four-LED indoor MIMO-VLC system was considered again, and the elevation angle was set at 35 degrees. GADR is still advantageous in low SNR regions, but the breakpoint drops from *115 dB* to *105 dB* at the location of *Position 6*. Since the receiver is located in the center of the room and achieves *4x4* symmetry, SMP performance approaches adaptive schemes in the high SNR region.

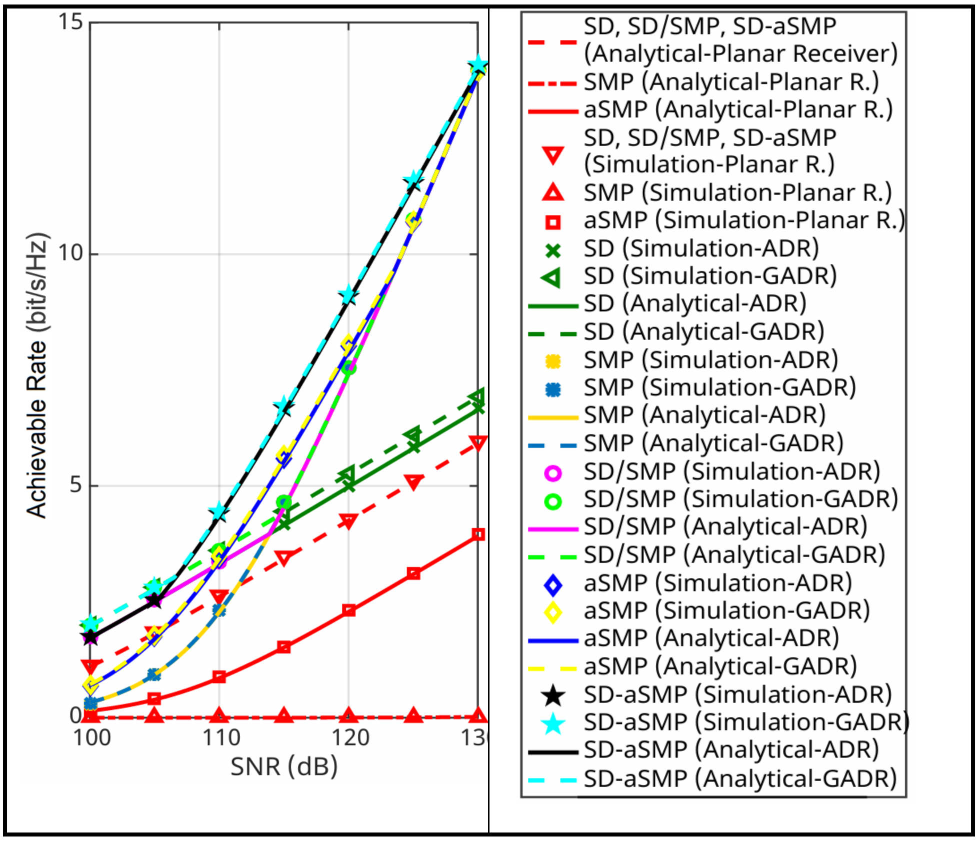

Figure 5. *Achievable rates of 4x4 and 4x5 MIMO-VLC schemes considering all receivers at Position 6.*

In Figure 6, the graph shows the achievable rate of *8x9* MIMO-VLC schemes with GADR at *Position 1*. The elevation angle was selected as *45* degrees. Marks and lines indicate the simulation and analytical findings, respectively. The simulations match closely with the analytical results. SD-aSMP and aSMP show superior performance as SNR increases compared to other schemes. While SD and SD-aSMP have the same performance in the low SNR region up to *110* dB, after this value the performance difference increases exponentially in favor of SD-aSMP, the dominant factor now is the multiplexing gain.

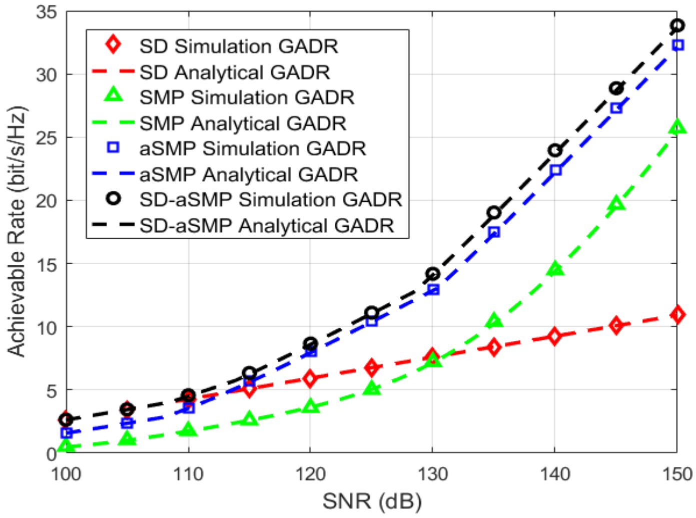

Figure 6. *Achievable rate of 8x9 MIMO-VLC schemes with GADR at Position 1.*

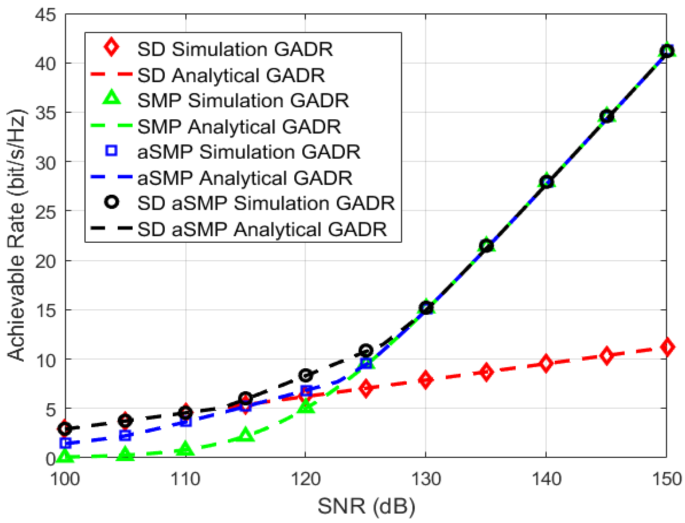

Figure 7. *Achievable rate of 8x9 MIMO-VLC schemes with GADR at Position 3.*

The performance difference between conventional and adaptive MIMO schemes increases at *Position 1*, especially at high SNR values. Weak signal paths that degrade traditional MIMO performance are combined in adaptive MIMO schemes by sending the same signal. Hence, this feature leads to improved performance.

In Figure 7, the elevation angle was set at *45* degrees, similar to Figure 6. Figure 7 displays the achievable rate of *8x9* MIMO-VLC schemes with GADR at *Position 3*. All SMP and its variations' performances get closer to each other as the SNR increases, and they all outperform SD. *Position* 3 is located away from the corner, and the signal strengths of the different paths are nearly similar. Therefore, the SD-aSMP, aSMP, and SMP performances are closely matched in the high SNR region.

4.1. CDF of Achievable Rates for MIMO-VLC

The data on achievable rates was collected at 1849 positions in the room to generate CDF graphs. The receiver unit moves around the room 40 cm away from the walls, with a 10 cm gap between each measurement. In Figure 8, we have conducted CDF plots to illustrate the achievable rates using SD, SMP, and SD-aSMP for elevation angles of *30, 45*, and *60* degrees under *120* dB transmit SNR conditions. The considered MIMO-VLC setup has *8* LEDs at the ceiling and GADR at the receiver. If we consider the half of the room corresponding to the CDF value of *0.5*, the achievable rate decreases as the elevation angle increases for the SD scheme. However, this trend is reversed for the SMP, where an increasing elevation angle leads to a higher achievable rate. In the case of SD-aSMP, increasing the elevation angle from 30^o to 45^o results in a significant performance improvement, but there is no meaningful change when the angle is increased from $45°$ to $60°$ for the CDF value of *0.5*. Moreover, considering *90%* of the room, improvement occurs as the elevation angle increases. Consequently, we can say that the increasing elevation angle reduces the total power received, lowers the SNR, and SD performance decreases throughout the room. For SMP and SD-aSMP, the situation is exactly the opposite. Increasing the elevation angle up to 60^o increases performance throughout the room by reducing inter-channel correlation. In this particular case, it is worth noting that the SD-aSMP demonstrates nearly the same performance at both elevation angles of *45* and *60* degrees, due to its hybrid structure. Ultimately, the optimal performance is attained by employing the SD-aSMP scheme with an elevation angle of *60* degrees.

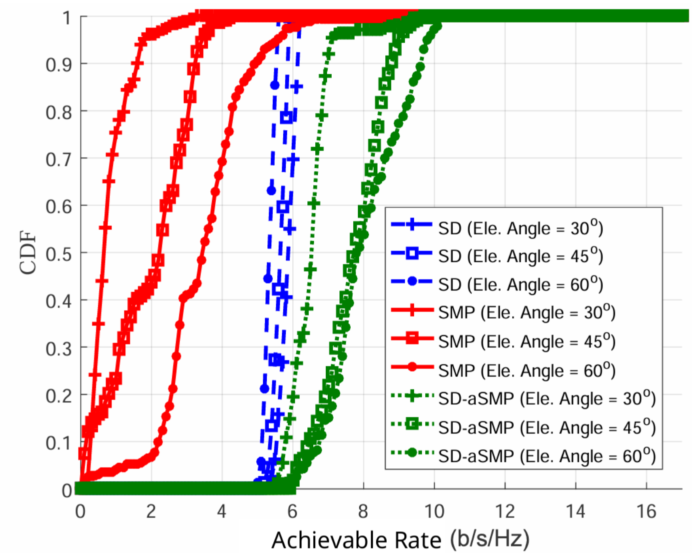

Figure 8. *CDF of achievable rates for 8x9 MIMO-VLC schemes with GADR.*

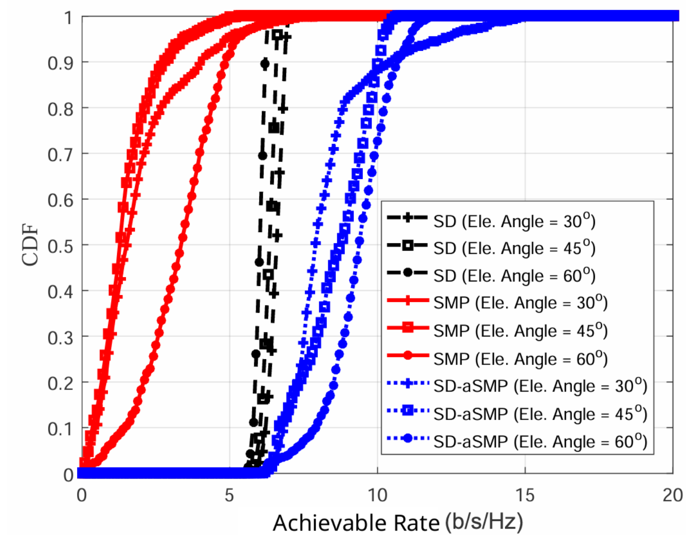

Figure 9. *CDF of achievable rates for 12x13 MIMO-VLC schemes with GADR.*

In Figure 9, the CDF of achievable rates is shown for *12x13* MIMO-VLC schemes with GADR considering the entire room. The performance of SMP and SD-aSMP improved throughout the room compared to the *8x9* MIMO-VLC setup, but the SD performance is almost the same. Multiplexing increases throughput linearly with the number of LEDs in the case of SMP and SD-aSMP. However, if the total power is fixed, increasing the number of LEDs does not improve the SD performance. The SMP and SD-aSMP achieve the best performance with an elevation angle of *60* degrees at the receiver. As an exception, SD-aSMP with an elevation angle of *30* degrees at the receiver achieves the best performance in *8%* of the room. The CDF of achievable rates for *16x17* MIMO-VLC schemes is displayed in Figure 10 when the GADR is utilized at the receiver. SD-aSMP achieves the best performance in 28% of the room when the receiver has an elevation angle of *30* degrees; *60* degrees works best in the rest of the room. Finally, considering three different LED setups, it is worth noting that SD outperforms SMP, and SD-aSMP outperforms SD for all elevation angles.

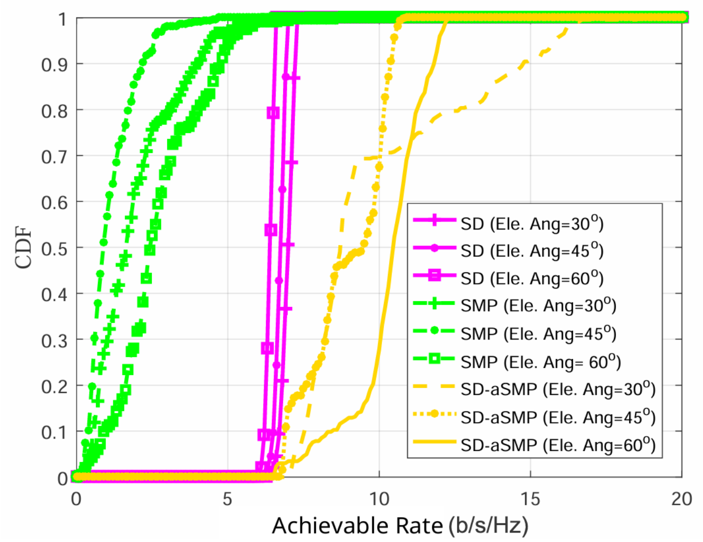

Figure 10. *CDF of achievable rates for 16x17 MIMO-VLC schemes with GADR.*

5. CONCLUSION

In this paper, the performance of an indoor adaptive MIMO-VLC system was evaluated by examining the achievable data rates with ADR and GADR receivers.

Achievable data rate performances were evaluated based on SNR at various positions, with simulation and analytical results being obtained and compared. It was found that GADR outperformed ADR in low SNR regions but performed similarly in high SNR regions. The SD-aSMP scheme demonstrated the best performance across all SNR regions, leveraging diversity gain in low SNR and multiplexing gain in high SNR regions. SMP with a planar receiver has the worst performance. The adaptive SMP schemes benefit from increasing the number of LEDs.

CDF graphs were generated by collecting data at 1849 positions in the room, examining the performance of SD, SMP, and SD-aSMP schemes at various elevation angles. Higher elevation angles improved the performances of SMP and SD-aSMP but decreased SD performance. The best overall performance was achieved with the SD-aSMP scheme at a 60^o angle. In conclusion, user-centric MIMO-VLC systems greatly enhance indoor communication performance by utilizing angular diversity receivers to improve weak signal paths which results in significant performance gains, particularly in high SNR regions.

CONFLICT OF INTEREST STATEMENT

The authors declare no conflict of interest.

REFERENCES

Alsabah, M., et al. (2021) “6G Wireless Communications Networks: A Comprehensive Survey”. *IEEE Access*, Vol. 9, pp. 148191-148243. doi: 10.1109/ACCESS.2021.3124812.

Armstrong, J. (2009). “OFDM for Optical Communications”. *Journal of Lightwave Technology*, 27(3), pp. 189-204. doi: 10.1109/JLT.2008.2010061.

Armstrong, J. & Schmidt, B. J. C. (2008) “Comparison of Asymmetrically Clipped Optical OFDM and DC-Biased Optical OFDM in AWGN”. *IEEE Communications Letters*, 12(5), pp. 343-345. doi: 10.1109/LCOMM.2008.080193.

Armstrong, J., Sekercioglu, Y. A., & Neild, A. (2013). “Visible light positioning: a roadmap for international standardization”. *IEEE Communications Magazine*, 51(12), pp. 68-73. doi: 10.1109/MCOM.2013.6685759.

Celik, Y. (2023). “Location-Based Visible Light Communication”. *31st Signal Processing and Communications Applications Conference (SIU)*, Istanbul, Turkiye. doi: 10.1109/SIU59756.2023.10223907.

Chen, C., Yang, H., Du, P., Zhong, W.-D., Alphones, A., Yang, Y., & Deng, X. (2020). “User-centric MIMO techniques for indoor visible light communication systems”. *IEEE Systems Journal*, 14(3), pp. 3202–3213. doi: 10.1109/JSYST.2019.2961696.

Chen, Z., Basnayaka, D.A. & Haas, H. (2017). “Space division multiple access for optical attocell network using angle diversity transmitters.” *Journal of Lightwave Technology*, 35, pp. 2118–2131. doi: 10.1109/JLT.2017.2670367.

Dixit, V. & Kumar, A. (2020). “Performance analysis of indoor visible light communication system with angle diversity transmitter.” *In Proceedings of the IEEE fourth Conference on Information & Communication Technology (CICT)*, Chennai, India, 3–5 December 2020, pp. 1–5. doi: 10.1109/CICT51604.2020.9312087.

Fath, T. & Haas, H. (2013). “Performance Comparison of MIMO Techniques for Optical Wireless Communications in Indoor Environments”. *IEEE Transactions on Communications*, 61(2), pp. 733-742. doi: 10.1109/TCOMM.2012.120512.110578.

Gesbert, D., Shafi, M., Shiu, D., Smith, P. J. & Naguib, A. (2003). "From theory to practice: an overview of MIMO space-time coded wireless systems". *IEEE Journal on Selected Areas in Comm.*, 21(3), pp. 281-302. doi: 10.1109/JSAC.2003.809458.

Guo, F., Yu, F. R., Zhang, H., Li, X., Ji, H. & Leung, V. C. M. (2021). "Enabling Massive IoT Toward 6G: A Comprehensive Survey". *IEEE Internet of Things Journal*, 8(15), pp. 11891-11915. doi: 10.1109/JIOT.2021.3063686.

Harada, R., Geldard, C. T. & Popoola, W. O. (2023). "Performance Analysis of Angular Diversity Receivers in Visible Light Communications". *IEEE 34th Annual International Symposium on Personal, Indoor and Mobile Radio Communications (PIMRC)*, Toronto, ON, Canada. doi: 10.1109/PIMRC56721.2023.10294068.

Horunlu, K. & Celik, Y. (2024). "User-Centric Visible Light Communication," *32nd Signal Processing and Communications Applications Conference (SIU)*, Mersin, Turkiye, pp. 1-4, doi: 10.1109/SIU61531.2024.10600789.

Kahn, J. M. & Barry, J. R. (1997). "Wireless infrared communications". *Proceedings of the IEEE*, 85(2), pp. 265-298. doi: 10.1109/5.554222.

Luo, P. et al., (2015). "Experimental Demonstration of RGB LED-Based Optical Camera Communications", *IEEE Photonics Journal*, 7(5), pp. 1-12. doi: 10.1109/JPHOT.2015.2486680.

Nuwanpriya, A., Ho, S. -W., & Chen, C. S. (2014). "Angle diversity receiver for indoor MIMO visible light communications". *IEEE Globecom Workshops (GC Wkshps)*, Austin, TX, USA. doi: 10.1109/GLOCOMW.2014.7063472.

Nuwanpriya, A., Ho, S. -W., & Chen, C. S. (2015). "Indoor MIMO Visible Light Communications: Novel Angle Diversity Receivers for Mobile Users". *IEEE Journal on Selected Areas in Communications*, 33(9), pp. 1780-1792. doi: 10.1109/JSAC.2015.2432514.

Qin, B., Wen, W., Liu, M., Zhang, Y. & Chen C. (2022). "Indoor MIMO-VLC Using Angle Diversity Transmitters." *Sensors*, 22(14), pp. 5436. doi: 10.3390/s22145436.

Penrose, R. A. (1955). "Generalized inverse for matrices". *Mathematical Proceedings of the Cambridge Philosophical Society*. 51(3) pp. 406-413. doi: 10.1017/S0305004100030401.

Shannon, C. E. (1948). "A mathematical theory of communication". *The Bell System Technical Journal*, 27(3), pp. 379-423. doi: 10.1002/j.1538-7305.1948.tb01338.x.

Su, Y., et al. (2024). "Efficient User-Centric AP Clustering Through Stable UE-AP Matching for Indoor VLC Systems," *IEEE Wireless Communications Letters*, 13(7), pp. 1903-1907. doi: 10.1109/LWC.2024.3395511.

Tanaka, Y., Komine, T., Haruyama S. & Nakagawa, M. (2001) "Indoor visible communication utilizing plural white LEDs as lighting". *12th IEEE International Symposium on Personal, Indoor and Mobile Radio Communications. PIMRC 2001*, San Diego, CA, USA doi: 10.1109/PIMRC.2001.965300.

Telater, I.E. (1999). "Capacity of multi-antenna Gaussian channels". *European Transactions on Telecomm.*, 10(6), pp. 585-595. doi: 10.1002/ett.4460100604.

Tsonev, D., Videv, S., and Haas, H. (2014). "Light fidelity (Li-Fi): towards all-optical networking", *Proc. SPIE 9007, Broadband Access Communication Technologies VIII*, 900702. doi: 10.1117/12.2044649.

Vegni, A. M. & Biagi, M. (2019). "Optimal LED placement in indoor VLC networks". *Optics Express*, 27(6), pp. 8504-8519. doi: 10.1364/OE.27.008504.

Yesilkaya, A., Basar, E., Miramirkhani, F., Panayirci, E., Uysal, M. & Haas, H. (2017). "Optical MIMO-OFDM with generalized LED index modulation," *IEEE Trans. Commun.*, 65(8), pp. 3429–3441. doi: 10.1109/TCOMM.2017.2699964.

Zeng, L., et al. (2009). "High data rate multiple input multiple output (MIMO) optical wireless communications using white led lighting". *IEEE Journal on Selected Areas in Comm.*, 27(9), pp. 1654-1662. doi: 10.1109/JSAC.2009.091215.

Zhang, J., Björnson, E., Matthaiou, M., Ng, D. W. K., Yang, H. & Love, D. J. (2020). "Prospective Multiple Antenna Technologies for Beyond 5G," *IEEE Journal on Selected Areas in Comm.*, 38(8), pp. 1637-1660. doi: 10.1109/JSAC.2020.3000826.